Sulcal Morphometry Predicts Mild Cognitive Impairment Conversion to Alzheimer's Disease

Giovanni Sighinolfi[a,1], Micaela Mitolo[a,b,1], Fabrizio Pizzagalli[c], Michelangelo Stanzani-Maserati[a],
Daniel Remondini[d], Magali Jane Rochat[a], Elena Cantoni[a], Greta Venturi[a], Gianfranco Vornetti[a,e],
Fiorina Bartiromo[a], Sabina Capellari[a,e], Rocco Liguori[a,e], Caterina Tonon[a,e,*], Claudia Testa[d,1]
and Raffaele Lodi[a,e,1]
[a]IRCCS Istituto delle Scienze Neurologiche di Bologna, Bologna, Italy
[b]Department of Medicine and Surgery, University of Parma, Parma, Italy
[c]Department of Neurosciences, University of Turin, Turin, Italy
[d]Department of Physics and Astronomy, University of Bologna, Bologna, Italy
[e]Department of Biomedical and Neuromotor Sciences, University of Bologna, Bologna, Italy

Abstract.
Background: Being able to differentiate mild cognitive impairment (MCI) patients who would eventually convert (MCIc) to Alzheimer's disease (AD) from those who would not (MCInc) is a key challenge for prognosis.
Objective: This study aimed to investigate the ability of sulcal morphometry to predict MCI progression to AD, dedicating special attention to an accurate identification of sulci.
Methods: Twenty-five AD patients, thirty-seven MCI and twenty-five healthy controls (HC) underwent a brain-MR protocol (1.5T scanner) including a high-resolution T1-weighted sequence. MCI patients underwent a neuropsychological assessment at baseline and were clinically re-evaluated after a mean of 2.3 years. At follow-up, 12 MCI were classified as MCInc and 25 as MCIc. Sulcal morphometry was investigated using the BrainVISA framework. Consistency of sulci across subjects was ensured by visual inspection and manual correction of the automatic labelling in each subject. Sulcal surface, depth, length, and width were retrieved from 106 sulci. Features were compared across groups and their classification accuracy in predicting MCI conversion was tested. Potential relationships between sulcal features and cognitive scores were explored using Spearman's correlation.
Results: The width of sulci in the temporo-occipital region strongly differentiated between each pair of groups. Comparing MCIc and MCInc, the width of several sulci in the bilateral temporo-occipital and left frontal areas was significantly altered. Higher width of frontal sulci was associated with worse performances in short-term verbal memory and phonemic fluency.
Conclusions: Sulcal morphometry emerged as a strong tool for differentiating HC, MCI, and AD, demonstrating its potential prognostic value for the MCI population.

Keywords: Alzheimer's disease, brain sulci, cortical thickness, MCI conversion, mild cognitive impairment, sulcal morphometry

---

[1]These authors contributed equally to this work.

*Correspondence to: Prof. Caterina Tonon, Functional and Molecular Neuroimaging Unit, IRCCS Istituto delle Scienze Neurologiche di Bologna – AUSL BO, Bellaria Hospital, Via Altura 3, 40139 Bologna, Italia. Department of Biomedical and Neuromotor Sciences, University of Bologna, Via Massarenti 9, 40138 Bologna, Italia. E-mail: caterina.tonon@unibo.it.

INTRODUCTION

Mild cognitive impairment (MCI) is an intermediate clinical stage between the expected cognitive decline of normal aging and the very earliest features of dementia [1]. In the last years, while a large body of literature focused on the early diagnosis of MCI

[2], only few studies have investigated with advanced magnetic resonance imaging (MRI) techniques the specific features that may support distinguishing "MCI due to Alzheimer's Disease (AD)" from the other MCI subgroups thus predicting the progression from MCI to dementia. There is converging evidence that a combination of clinical, neuropsychological, and multimodal neuroimaging findings may give useful information at the MCI stage to early identify the prodromal AD cases. However, distinguishing MCI 'converter' from those MCI that will remain stable over time (i.e., MCI 'non-converter') is still a matter of debate.

A recent study [3] investigated the valence of proton magnetic resonance spectroscopy (^{1}H-MRS) combined with brain volumetry to detect early metabolic and morphometric changes in MCI patients thus possibly predicting a progression to AD. Results confirmed a high accuracy of both N-acetyl-aspartate (NAA, neuro-axonal marker), and myo-Inositol (mI, glial marker) ratio and volume of parahippocampal gyrus in predicting the conversion to AD about two years before the development of clinical symptoms. Similar approaches combining metabolic and structural features have also been proven to have the capability of differentiating diverse types of dementia [4]. In the large body of literature available on AD and MCI, neuropsychological performances have been associated to brain functional and morphometric alterations such as volume or thickness reduction of specific brain cortical and subcortical structures; however, only few studies have examined the association with cortical surface anatomy such as sulci features [5, 6]. Since brain atrophy has been largely associated with the progression of dementia [7], we can expect that the increase of the inter-gyral space, and thus sulci changes may provide accurate biomarker of MCI conversion to AD. Indeed Bertoux and colleagues [8] showed that sulcal width better classified AD patients compared to cortical thickness.

Previous studies of sulcal-based morphometry showed that folding patterns were modified in certain professional groups, such as musicians [9], but also in psychiatric syndromes [10–14] and neurodegenerative disorders [8, 15, 16]. Other studies on healthy adults have found that the width of cortical sulci expands linearly with aging [5, 17, 18] and that the sulci widening process is different between males and females [19]. The average sulcal width in the frontal lobe was found to be negatively associated with some cognitive function in healthy elderly individuals such as processing speed [20, 21]. Additionally, the sulcal width of temporal regions and the anterior cingulate cortex was recently demonstrated to be negatively associated with cognitive performance [22]. Lately, various studies have described an increased width of frontal and temporal sulci in patients with MCI or AD [8, 16, 23, 24]. A study investigating gyri and sulci features in patients with AD found that global cortex gyrification decreased with the increasing severity of AD [25].

Although the increasing volume of literature exploring the value of sulci morphometry as a parameter to study the brain architecture and to correlate with pathological conditions, much has still to be done to validate its value and its potentiality in diagnosis and prognosis assessment. In particular, the high inter-subject variability in sulcal morphometry has led in some cases to inconsistent findings which induces to find approaches in the processing of brain data able to minimize the effects of inter-individual variations.

The aim of this study was to investigate the ability of sulcal morphometry and cortical thickness to predict the progression from MCI to AD, based on clinical classification at about two-years follow-up, and to explore their correlations with neuropsychological performance. We hypothesized that the sulcal features that better discriminate those MCI that will convert to AD from non-converter MCI, are also correlated to worse cognitive performance. Special attention was devoted to verify and manually correct, when needed, the classification of sulci at the level of single nodes in each subject to achieve an accurate identification. This procedure was not performed in previous studies [8, 16, 23–27].

METHODS

Participants

Eighty-seven subjects were retrospectively included in this study. Among them, thirty-seven were MCI patients (19 males, age 73.9 ± 7.4 years, range 52-84 years; mean level of education 7.3 ± 3.8 years), twenty-five were AD patients (15 males, age 70.8 ± 9.3 years, range 51-84 years; mean level of education 8.4 ± 3.9 years), and twenty-five were healthy controls (11 males, age 68.4 ± 9.2 years, range 52-83 years) with no neurological or psychiatric disease reported.

The MCI patients were classified as 'multi-domain', either amnestic or non-amnestic and the mean disease duration was 12.0 ± 1.2 months;

instead the mean disease duration of the AD group was 24.1 + 1.5 months.

All patients were consecutively referred between 2009 and 2018 to the Functional MR Unit, S.Orsola-Malpighi Hospital, Bologna (IT), to perform brain MR investigation as part of the diagnostic workup. Healthy controls were selected from the Neuroimaging Laboratory database of healthy volunteers (Ethical Committee approval Cod.: 120/2014, 7.10.2014).

The clinical condition of patients was assessed by neurologists experienced in neurodegenerative disorders, according to international criteria for MCI [28] and AD [29]. The maximum interval between the clinical assessment at baseline and the MR scan was three months.

All included participants did not show evidence of any psychiatric disease, major depression, or history of any other clinically significant diseases.

Clinical and neuropsychological evaluation of MCI patients was performed at baseline and clinical evaluation was repeated after an average of 28 ± 15 months. At follow-up, all MCI patients that evolved to Parkinson's disease, frontotemporal dementia, Lewy bodies disease or to any other neurodegenerative disorders different from AD were excluded from the study and are not counted in the final cohort of 37 MCI subject. Based on the clinical follow-up, 25 MCI patients were classified as converter (13 males, age 73.6 ± 7.1 years, range 54-84 years) and 12 as non-converter (6 males, age 74.0 ± 7.9 years, range 67-84 years). Main demographic and clinical characteristics of the study group are reported in Table 1.

All subjects gave consent to personal data processing for research purposes and the protocol was approved by the local Ethical Committee (v. 1.0 April 2010).

The same cohort of participants, with the exclusion of one MCI patient, due to the failed reconstruction of sulci, and the addition of seven healthy controls, was previously studied by Mitolo and colleagues [3] to investigate the ability of volumetric and spectroscopic features to predict the progression from MCI to AD on the basis of clinical classification at follow-up.

Neuropsychological assessment

A complete neuropsychological assessment of MCI at baseline was performed. For a detailed description of the scales used, see Mitolo and colleagues [3].

MRI protocol acquisition

Brain MR studies were performed using a 1.5 Tesla system (GE Medical Systems Signa HDx 15) equipped with a quadrature birdcage head coil. Structural imaging included 3D volumetric T1-weighted FSPGR images (TR = 12.5 ms, TE = 5.1 ms, TI = 600 ms, 25.6 cm^2 FOV, 1 mm^3 isotropic voxels), axial FLAIR T2-weighted images (TR = 8000 ms, TI = 2000 ms, TE = 93.5 ms, 4 mm slice thickness with no inter-slice gap), and FSE coronal T2-weighted images (TR = 7000 ms, TE = 100 ms, 4 mm slice thickness). Brain MR images obtained from each subject were visualized by a neuroradiologist with more than 30 years expertise (RL) in order to evaluate quality of images (such as motion artifacts) and exclude significant abnormalities in healthy controls.

MRI pre-processing

The evaluation of sulcal morphometry was performed following the ENIGMA-Sulci protocol (http://enigma.ini.usc.edu/protocols/imaging-protocols/), described in [30, 31], which is based on the freely accessible BrainVISA 4.5 framework (https://brainvisa.info/web/index.html), including the Morphologist software [32–34].

The pre-processing of structural images consisted of the correction of intensity inhomogeneities and the segmentation of the brain structures, performed using FreeSurfer 5.3.0 (https://surfer.nmr.mgh.harvard.edu/).

Table 1
Main characteristics of the study groups

	HC ($n = 25$)	MCInc ($n = 12$)	MCIc ($n = 25$)	AD ($n = 25$)
Sex (M/F)	11/14	6/6	13/12	15/10
Age (y)	68.4 ± 9.2	74.0 ± 7.9	73.6 ± 7.1	70.8 ± 9.3
Follow-up (mo)	–	29 ± 22.6	27.1 ± 11.8	–

HC, healthy controls; MCInc, non-converter MCI patients; MCIc, converter MCI patients; AD, Alzheimer's disease patients.

The morphologist software was run on the pre-processed images including the FreeSurfer segmentation for sulcal extraction, identification, and sulcal-based morphometry of a total of 123 sulci (62 in the left and 61 in the right hemisphere) from the human cerebrum, according to the BrainVISA atlas (https://brainvisa. info/web/_static/images/bsa/nomenclature.png). Following the identification of sulci, the morphologist software provides for each sulcus a set of morphological descriptors in the individual-subject space, i.e., the surface area, the mean depth, the length and the width (or fold opening), which were used as input data for the statistical analysis. The length of a sulcus corresponds to the number of voxels on the junction between a sulcus and the hull of the brain. The mean depth is measured as the average of the geodesic distance along the bottom of the sulcus to the brain hull. The surface area is the total area of the sulcal surface. The mean width is derived as the enclosed CSF volume divided by the sulcal surface area [35, 36]. In the following, the abbreviations used to refer to sulci correspond to those of the atlas.

Data quality control and manual correction

Before retrieving the morphometric properties of sulci, a quality control was performed, as suggested both by BrainVISA (https://brainvisa.info/axon-5.1/en/processes/morphologist.html) and the ENIGMA-Sulci protocol (http://enigma.ini.usc.edu/protocols/imaging-protocols/) the labeling of each of the 123 sulci in every subject was visually inspected by two independent operators, using the Anatomist toolbox (https://brainvisa.info/web/anatomist.html). Whenever a sulcus was not properly identified by the automatic algorithm, its classification was manually modified according to the BrainVISA atlas. Since the Morphologist segmentation is designed to identify up to 5 types of elementary structures within a cortical fold, a sulcus is typically constituted by a set of "nodes" [37], which are then labelled by the tool as part of a specific sulcus, based on a probability map. The correction of the classification was performed at the level of single nodes, in order to achieve an accurate identification.

The labeling of the superior temporal sulcus (S.T.s.) and its rami (the anterior and posterior terminal ascending branch of the superior temporal sulcus, S.T.s.ter.asc.ant. and S.T.s.ter.asc.post.) was particularly challenging, as their morphology exhibits a prominent inter-subject variability. Two

experienced neuroradiologists (RL and FB), basing on a previous paper by Segal and colleagues [38], developed a standardized procedure to classify sulci in the posterior temporo-occipital area onto the BrainVISA atlas. The first sulcus posterior to the lateral fissure (F.C.L.p.) and originating from the temporal lobe, coursing towards the intraparietal sulcus (F.I.P.), was defined as the anterior ramus of the S.T.s. (S.T.s.ter.asc.ant.); moving towards the occipital lobe, the second sulcus originating in proximity of the termination of the S.T.s., was classified as the posterior ramus of the superior temporal sulcus (S.T.s.ter.asc.post.); the "posterior branch", as it is defined by Segal and colleagues [38], i.e., the ramus at the boundary between the occipital and the temporal lobe, was partially labeled as inferior temporal sulcus (S.T.i.post.) in its temporal portion, and as part of the occipital sulci (OCCIPITAL) at the strict boundary between the two lobes in the superior part, which points towards the parieto-occipital fissure. See Fig. 1 for an example of sulcal identification before and after relabeling. In the fold recognition step, it could also occur that cortical folds including different sulci were contiguous, so that the software recognized the fold as an individual structure and was not able to properly separate it into different nodes. To overcome this misclassification and achieve improved consistency, before the statistical analysis, the sulci exhibiting such issue were merged into a unique one. The S.T.s. with one of its anterior or posterior branches was one of the most common cases where the separation failed; because of this, it was not possible to distinguish all the different portions of the superior temporal sulci in each subject. For analogous reasons, the following sulci (referring to the BrainVISA nomenclature) were merged prior to the statistical analysis: the inferior and intermediate precentral sulci (S.Pe.C.inf., S.Pe.C.inter.); the superior, marginal, and median precentral sulci (S.Pe.C.sup., S.Pe.C.marginal., S.Pe.C.median.); the superior and inferior postcentral sulci (S.Po.C.sup., F.I.P.Po.C.inf.); the intraparietal sulcus and its rami (F.I.P., F.I.P.r.int.1, F.I.P.r.int.2); the complete list is reported in Table 2. Additionally, given the poor recognizability in each subject of the supramarginal sulcus (S.GSM.) in the left hemisphere, it was removed from further analysis. Therefore, the total number of sulci included in the statistical analysis was 106.

Lastly, due to the high inter-subject variability of sulcal morphology, certain minor sulci (such as the sub-central rami of the lateral fissure) were not
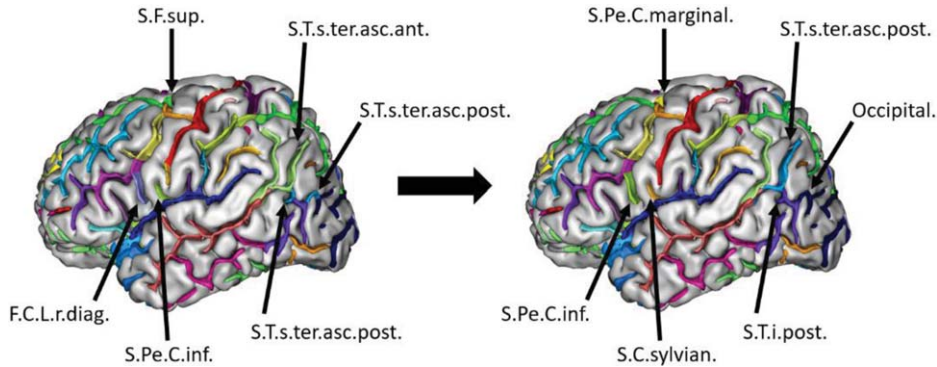
Fig. 1. Example of the relabeling performed on sulcal nodes in the left hemisphere of a converter MCI patient. The colors correspond to those of the BrainVISA atlas. The anterior and posterior branches of the superior temporal sulcus (S.T.s.) were relabeled, as well as a portion of the posterior inferior temporal suclus (S.T.i.post.) and the occipital sulcus; in the frontal area, the classification of the central sylvian sulcus (S.C.sylvian.) and the inferior precentral sulcus (S.Pe.C.inf) were corrected. S.F.sup., superior frontal sulcus; S.T.s.ter.asc.ant., anterior terminal ascending branch of the superior temporal sulcus; S.T.s.ter.asc.post., posterior terminal ascending branch of the superior temporal sulcus; S.Pe.C.inf., inferior precentral sulcus; F.C.L.r.diag., diagonal ramus of the lateral fissure; S.Pe.C.marginal., marginal precentral sulcus.

Table 2
List of cerebral sulci that were merged before performing the analysis, due to the frequent misclassification of the automatic algorithm

Merged sulci	Output sulcus
S.T.s., S.T.s.ter.asc.ant., S.T.s.ter.asc.post.	S.T.s.
S.Pe.C.inf., S.Pe.C.inter.	S.Pe.C.inf.
S.Pe.C.sup., S.Pe.C.marginal., S.Pe.C.median.	S.Pe.C.sup.
F.I.P.Po.C.inf., S.Po.C.sup.	S.Po.C.
F.I.P., F.I.P.r.int.1, F.I.P.r.int.2	F.I.P.

S.T.s., superior temporal sulcus; S.T.s.ter.asc.ant., anterior terminal ascending branch of the superior temporal sulcus; S.T.s.ter.asc.posterior., posterior terminal ascending branch of the superior temporal sulcus; S.Pe.C.inf., inferior precentral sulcus; S.Pe.C.inter., intermediate precentral sulcus; S.Pe.C.sup., superior precentral sulcus; S.Pe.C.marginal., marginal precentral sulcus; S.Pe.C.median., median precentral sulcus; F.I.P.Po.C.inf., inferior postcentral sulcus; S.Po.C.sup., superior postcentral sulcus; F.I.P., intraparietal sulcus; F.I.P.r.int.1, primary intermediate ramus of the intraparietal sulcus; F.I.P.r.int.2, secondary intermediate ramus of the intraparietal sulcus.

identifiable in all subjects, and they were therefore under-represented in the data, even though they were maintained for the following analysis.

These sulci, as well as the ones that most frequently required re-labeling, mostly corresponded to the ones classified as unreliable in the paper by Pizzagalli and colleagues [30], basing on the automatic sulcal recognition performed by BrainVISA.

Analysis of cortical thickness

The evaluation of the cortical thickness of 35 regions from the Desikan-Killiany atlas [39] per hemisphere was achieved by applying the FreeSurfer

5.3.0 segmentation on the 3D T1 images. Quality control was performed via visual inspection of the results. Note that, even though there is not a unique correspondence between the cortical regions defined by FreeSurfer and the sulci identified by BrainVISA, there clearly exists a non-exclusive morphological connection, since the two segmentations are partially overlapping and sulcal morphology is influenced by the underlying cortical anatomy.

Statistical analysis

The normality of the distribution of all parameters was tested using Shapiro-Wilk test. The age distribution between groups was compared using ANOVA and the gender distribution using Pearson's χ^2-test.

The same procedure for the statistical analysis was applied for each sulcal feature and for the cortical thickness of every region, using Matlab R2019a (9.6.0.1072779). All the quantitative MR parameters of each subject were adjusted for the Total Intracranial Volume (TIV), as measured with FreeSurfer 5.3.0, using the residual methods, which is reported to intrinsically account for the sex of the subject [40]. The non-parametric Mann-Whitney U test or Kruskal–Wallis test, followed by a pairwise Bonferroni post-hoc test for multiple comparisons, were used to compare each quantitative MR parameter between groups. Each feature that differed significantly between any pair of groups was used to fit a logistic model as a classifier and to calculate a Receiver Operating Characteristic (ROC) curve for the outcomes. The ROC analysis allowed us to extract

the Area Under Curve (AUC), the specificity, sensitivity and accuracy of the classification, basing on the optimal ROC point estimated through the Index of Union [41]. The same analysis was repeated correcting for the effects of age alone and age and sex combined, in addition to the TIV, and the results are reported in Supplementary Material, section 1 and 2 respectively. In the next section, results are reported only for the feature that achieved the best discrimination performance for each contrast, even though additional features have demonstrated good classification capabilities. As an exception, given the major importance of the classification of MCIc versus MCInc, all the statistically significant results for this comparison are reported.

As the size of the sample would not allow to build training and test sets, to assess the solidity of the outcomes, beside the in-sample analysis, the same procedure was repeated while performing a Leave-One-Out cross validation, where one subject's classification was predicted basing on the logistic fit obtained from the remaining individuals of the two groups taken into account.

Additionally, the classification performances of features that differed significantly between converter and non-converter MCI were evaluated using a multivariate approach. The data were fed to a 2D ISOMAP for dimensionality reduction [42] and the resulting features were used to classify the MCI patients into converter or non-converter with a Support Vector Machine (SVM) using a linear kernel and a Leave-One-Out Cross Validation.

Statistical significance was set at $p < 0.05$ after Bonferroni correction, taking into account 4×106 tests, that corresponds to the whole set of sulci (some of them merged as reported in Table 2) for the four measures.

Lastly, to analyze the association between brain structural properties and cognitive functions, Spearman's correlation coefficients were calculated between the morphometric properties that resulted to be significantly different when comparing MCIc with MCInc and the neuropsychological scores that MCI patients obtained at baseline.

RESULTS

Demographic, clinical, and neuropsychological data

At the clinical follow-up, performed after an average of 28 months from baseline, among the 37 MCI,

Table 3
Comparison of the baseline neuropsychological performance between the two subgroups of MCI. None showed statistically significant differences

Cognitive test	MCInc ($n = 12$)	MCIc ($n = 25$)	Uncorr p
MMSE	26.8 (2.4)	26.0 (2.8)	0.40
RAVLT – immediate	31.4 (10.3)	25.3 (7.5)	0.09
RAVLT – delayed	5.5 (3.5)	2.2 (3.0)	0.01
Visual memory	17.2 (3.4)	16.8 (3.7)	0.66
Analogies	15.0 (2.7)	13.6 (4.2)	0.35
Phonemic Fluency	27.0 (9.7)	24.5 (10.5)	0.53
Semantic Fluency	23.7 (6.1)	21.8 (7.3)	0.22
Stroop (time)	34.0 (10.9)	42.3 (21.8)	0.44
Stroop (error)	2.6 (3.2)	4.5 (6.5)	0.83
Barrage (time)	77.6 (26.7)	81.7 (40.2)	1
Barrage (error)	1.4 (1.2)	4,4 (5.9)	0.38
Barrage (P)	10.3 (1.9)	10.7 (2.0)	0.51
Copy drawing	9.4 (2.8)	9.5 (2.4)	1
BDI	12.0 (9.0)	12.8 (12.3)	0.97
STAI X1	41.1 (9.1)	44.4 (8.5)	0.70
STAI X2	38.8 (9.9)	41.9 (11.9)	0.67

$P < 0.003$ (correction per multiple comparisons); MMSE, Mini-Mental State Examination; RAVLT, Rey Auditory Verbal Learning Test; BDI, Beck Depression Inventory; STAI, State-Trait Anxiety Inventory.

25 patients converted to AD (MCIc, 13 males, age 73.6 ± 7.1 years), whereas 12 showed stable symptoms (MCInc, 6 males, age 74.0 ± 7.9 years). No significant differences of sex and age distribution were found between groups. The demographic characteristics of the MCI subgroups are reported in Table 1.

After Bonferroni correction, the two MCI subgroups did not exhibit any statistically significant difference in terms of the cognitive tests performed at baseline, as reported in Table 3.

All the structural MRI exams were of good quality. Healthy controls imaging did not show any morphological or signal intensity changes and the patients did not exhibit any changes suggesting any other neurological diseases.

Sulcal morphometry analysis

The need for relabeling was homogeneous across groups and sex and, on average, 8 sulci per subject were relabeled, at least partially. A schematic representation of the results obtained for each group, showing the 5 most discriminative sulci for each group comparison, is reported in Supplementary Figure 1. The cross validation returned AUC and accuracy values on average 2-4% lower with respect to the values of the in-sample analysis reported in this section (corresponding to about one patient not accurately

classified), suggesting the stability of the results and the robustness to overfitting of the analysis.

MCInc versus HC

Only few regions emerged as capable of discriminating MCInc from HC, and they were mostly located in the internal temporal area; among them, the most statistically significant property was the width of the left rhinal sulcus (S.Rh.), achieving a relatively low ROC AUC of 0.757 (corrected $p = 0.020$).

MCIc versus HC

The comparison between MCIc and HC exhibited more evident abnormalities, showing widespread alterations of sulcal surface and depth in the frontal, temporal and temporo-occipital areas, and of sulcal width across every lobe, with increased significance in the frontal and temporo-occipital areas; the most significant alteration emerged in terms of width of the left posterior occipito-temporal lateral sulcus (S.O.T.lat.post., ROC AUC = 0.941, corrected $p = 1 \cdot 10^{-7}$).

AD versus HC

Comparing AD with HC, similar outcomes emerged with respect to the contrast MCIc versus HC, but showing even more extended and significant regions of alterations for every morphometric property, also involving the parietal lobe. However, the most discriminating sulci were still located in the frontal, temporal and temporo-occipital areas, with the width of the left collateral fissure (F.Coll.) achieving the best result (ROC AUC = 0.947, corrected $p = 2 \cdot 10^{-8}$).

MCIc versus MCInc

When comparing MCInc and MCIc, sulcal surface, depth and length of few regions in the occipital, parietal and temporo-occipital areas were able to discriminate the subgroups, with the most significant one being the depth of right occipital sulci (ROC AUC = 0.833, corrected $p = 0.006$). Consistently with the other contrasts, the width showed the most significant and widespread outcomes, involving especially the left frontal and the bilateral temporal and temporo-occipital regions. For this feature, the most discriminating sulcus was the right posterior inferior temporal one (right S.T.i.post.) achieving a

Table 4

Sulci whose width is significantly higher in MCIc with respect to MCInc. The left frontal and bilateral posterior temporal areas exhibit the highest alterations

Sulcus	Width MCInc (mm)	Width MCIc (mm)	Corr p	AUC
Right S.T.i.post.	1.6 ± 0.2	2.1 ± 0.5	0.001	0.907
Left S.F.inter.	2.2 ± 0.4	2.9 ± 0.6	0.002	0.843
Left S.F.sup.	2.6 ± 0.4	3.3 ± 0.6	0.007	0.823
Left S.F.polaire.tr.	2.9 ± 1.2	3.8 ± 1.0	0.007	0.813
Left S.T.i.post.	1.7 ± 0.2	2.1 ± 0.4	0.012	0.880
Left S.O.T.lat.post.	1.7 ± 0.3	2.3 ± 0.6	0.011	0.853
Left S.O.T.lat.int.	1.7 ± 0.4	2.5 ± 0.9	0.033	0.800
Left S.Pe.C.inf.	2.5 ± 0.5	3.3 ± 0.8	0.043	0.792
Right S.Olf.	1.9 ± 0.4	2.8 ± 1.1	0.031	0.790
Left S.Olf.	2.0 ± 0.3	2.6 ± 0.9	0.044	0.787
Left S.F.int.	2.4 ± 0.6	3.0 ± 0.9	0.033	0.780
Right S.F.inter.	2.2 ± 0.5	2.6 ± 0.4	0.031	0.777
Right F.P.O.	1.9 ± 0.4	2.4 ± 0.5	0.031	0.777
Left S.R.inf.	1.6 ± 0.6	2.4 ± 0.8	0.043	0.769

S.T.i.post., posterior inferior temporal sulcus; S.F.inter., intermediate frontal sulcus; S.F.sup., superior frontal sulcus; S.F.polaire.tr., polar frontal sulcus; S.O.T.lat.post., posterior occipito-temporal lateral sulcus; S.O.T.lat.int., internal occipito-temporal lateral sulcus; S.Pe.C.inf., inferior precentral sulcus; S.Olf., olfactory sulcus; S.F.int., internal frontal sulcus; F.P.O., parieto-occipital fissure; S.R.inf., inferior rostral sulcus.

ROC AUC of 0.907, with a specificity of 0.917, sensitivity of 0.880, and accuracy of 0.892 (corrected $p = 0.001$), followed by the left intermediate frontal sulcus (left S.F.inter, ROC AUC = 0.843, specificity = 0.833, sensitivity = 0.840, accuracy = 0.838, corrected $p = 0.002$). All the statistically significant alterations are reported in Table 4 and Fig. 2.

The multivariate classification procedure demonstrated a good separability of the two groups using the features obtained via ISOMAP. Figure 3 shows the scatterplot of the data points of MCIc and MCInc patients along the two ISOMAP coordinates. The following classification performance achieved an accuracy = 0.865.

It is particularly interesting to note that the width of the right S.T.i.post. showed strong discriminant capabilities when comparing the states of absent/mild and severe dementia symptoms, as it can be seen from Fig. 4. Analogous outcomes were observed also for the left S.T.i.post. and the left S.F.inter.

AD versus MCInc

Comparing AD versus MCInc, in AD the temporal and occipital areas were mostly altered in terms of sulcal depth and width, even though the latter displayed widespread differences across all lobes; the
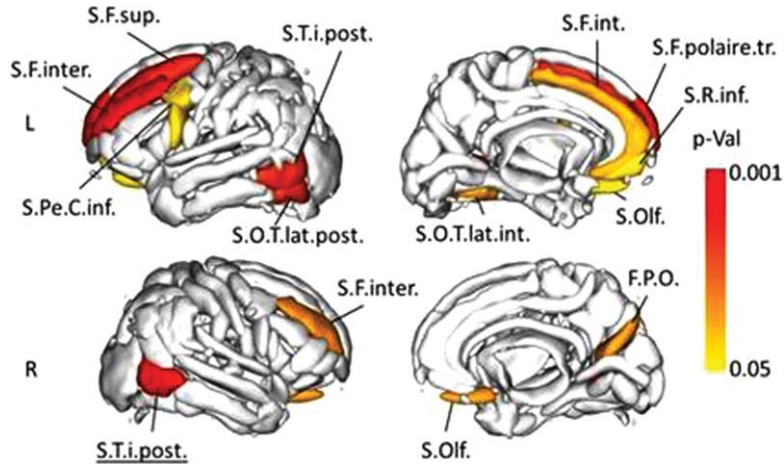
Fig. 2. Representation of the sulci whose width exhibited a statistically different value between MCIc and MCInc. The color intensity describes the significance of the result (MCIc > MCInc). S.T.i.post., posterior inferior temporal sulcus; S.F.inter., intermediate frontal sulcus; S.F.sup., superior frontal sulcus; S.F.polaire.tr., polar frontal sulcus; S.O.T.lat.post., posterior occipito-temporal lateral sulcus; S.O.T.lat.int., internal occipito-temporal lateral sulcus; S.Pe.C.inf., inferior precentral sulcus; S.Olf, olfactory sulcus; S.F.int., internal frontal sulcus; F.P.O., parieto-occipital fissure; S.R.inf., inferior rostral sulcus.
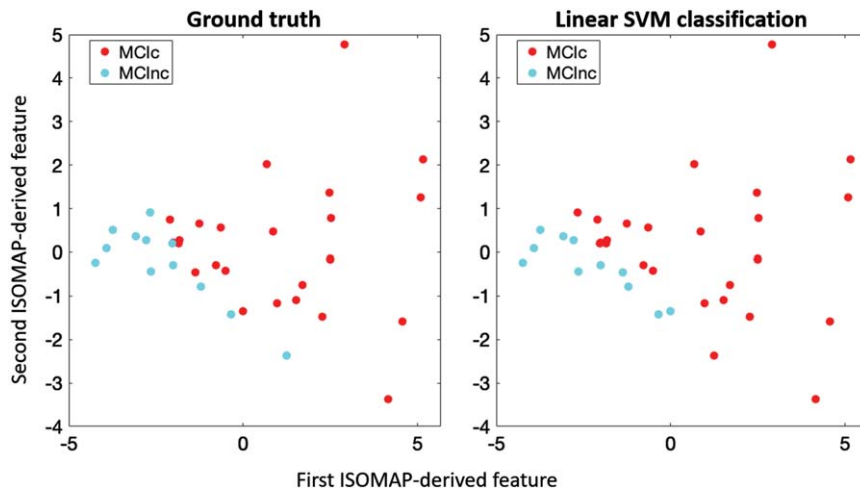

Fig. 3. Scatterplot representation of converter (MCIc, red) and non-converter MCI patients (MCInc, light blue) in the 2-dimensional reduced space retrieved by applying ISOMAP on the sulcal features. Left: Ground truth labelling of MCI; right: Linear support vector machine classification labelling: 5 out of 37 MCI patients were misclassified.

width of the right posterior inferior temporal sulcus (S.T.i.post.) was the most discriminating property (ROC AUC = 0.957, corrected $p = 1 \cdot 10^{-4}$).

AD versus MCIc

There were no sulcal features that differed significantly between MCIc and AD.

Cortical thickness analysis

The cortical thickness, which tended to decrease with the disease grade, exhibited in general worse dis-

criminating capabilities than the sulcal features (and the width in particular). There were no regions whose cortical thickness differed significantly between MCInc and HC.

Analogously to the results emerged from sulcal analysis, widespread alterations across different lobes were observed comparing MCIc and HC, while the most significant alterations were detected in the temporal area, and in particular the left entorhinal cortex achieved a ROC AUC of 0.818 ($p = 4 \cdot 10^{-4}$).

In AD versus HC, similarly to the previous case, abnormalities were diffused across all the brain cortex
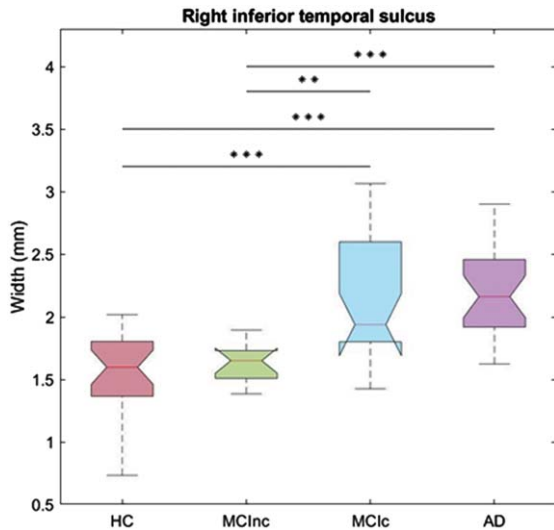
Fig. 4. Boxplot of the width of the right inferior temporal sulcus across the four groups. The feature evidently differentiates HC and MCI nc from AD and MCIc. **$p < 0.01$; ***$p < 0.001$. HC, healthy controls; MCInc, non-converter MCI; MCIc, converter MCI; AD, Alzheimer's disease.

and most prominent in the temporal area: the most significant one was the right inferior temporal cortex (ROC AUC = 0.884, $p = 2 \cdot 10^{-6}$).

There were no regions whose CT differed significantly between MCInc and MCIc.

Few alterations in the temporal area were able to distinguish AD from MCInc, and the most significant one was again the right inferior temporal cortex (ROC AUC = 0.827, $p = 0.03$). There were no regions whose CT differed significantly between AD and MCIc.

Correlation with neuropsychological scales

The sulcal features of surface, depth and length of any sulcus did not exhibit meaningful correlations with any of the neuropsychological scales.

Instead, the sulcal width exhibited significant correlations with specific NPS scores at baseline. In particular, the width of the right olfactory (S.Olf.) and the left inferior precentral (S.Pe.C.inf.) sulci had a negative relationship with the immediate Rey

Auditory Verbal Learning Test (RAVLT), a test that measured verbal short-term memory. In addition, the left S.Olf. negatively correlated with the delayed RAVLT (verbal long-term memory) and the right intermediate frontal sulcus with the phonemic fluency test, a test that measured verbal fluency involving also executive functions. Table 5 collects a summary of these results.

DISCUSSION

In this study, we described the characteristic alterations of the morphometry of cerebral sulci and cortical thickness in a group of HC, MCI, and AD patients. In particular, we detected and described those features that are capable of discriminating among these subgroups. A special focus was dedicated to the analysis of the properties that may predict those MCI patients who would eventually convert to AD, as opposed to those who would not. To achieve this, the morphological measures retrieved from sulci were evaluated at baseline for all patients, and they were compared between converter and non-converter MCI, as identified basing on a 2-year clinical follow-up.

Basing on the available literature, we expected progressively higher values of sulcal width [23–25] and lower depth [8], with the increasing severity of the patient condition, whereas the modification of length and surface was not trivially predictable. Additionally we expected the width to be the most discriminative measure [26, 27]. In our study, the sulcal features of surface, depth and length exhibited a decreasing trend with the disease grade, whereas the width showed an increment in MCIc and AD compared to HC and MCInc. The results showed that the sulcal width retains a high discriminating power in this cohort and achieves good results in classifying subjects belonging to the different subgroups. In particular, the width of various sulci in the inferior temporal (bilateral posterior inferior temporal sulcus), temporo-occipital (left internal and posterior temporo-occipital lateral sulci, right fronto-parietal sulcus) and frontal (bilat-

Table 5
Significant Spearman's correlation between the sulcal features and the neuropsychological scores obtained by MCI at baseline

Sulcal width	NPS scale	Correlation value	Uncorr p
Left inferior precentral sulcus	RAVLT (immediate)	−0.55	0.0007
Right olfactory sulcus	RAVLT (immediate)	−0.52	0.0015
Left olfactory sulcus	RAVLT (delayed)	−0.48	0.0038
Right intermediate frontal sulcus	Phonemic fluency	−0.48	0.0035

RAVLT, Rey Auditory Verbal Learning Test.

eral intermediate frontal and olfactory sulci; left superior, polar and internal frontal sulci; left precentral sulcus; left inferior rhinal sulcus) regions demonstrated excellent results in predicting the MCI conversion, as shown also via the multivariate representation of the data. The alterations in the inferior temporal and temporo-occipital region are consistent with the volumetric alterations reported in Mitolo and colleagues [3], where a reduction of the volume of the parahippocampal and fusiform gyri was described in the same cohort of patients. Additionally, the classification performances obtained using sulcal width were greater than those resulting from volumetric parameters.

The abnormality of sulcal morphometry, and the increment of sulcal width in the temporal and frontal areas described here is consistent with previous investigations of sulcal features in AD and MCI [8, 16, 23–27]. Additionally, a recent study by Mortamais and colleagues [22] suggests a positive association between sulcal widening in the temporal and cingulate regions and cognitive decline, even though the study was not restricted to AD or MCI patients. These studies found valuable discrimination capabilities and classification accuracy of sulcal width, in most cases superior to other typical morphological evaluations, such as volumetry or cortical thickness [8, 16, 23, 25]. Indeed, in our study, we observed that sulcal width achieved better outcomes than cortical thickness for each of the group comparisons performed. This is especially evident in the case of the comparison between MCIc and MCInc, where no alterations of cortical thickness were statistically significant. This result suggests that the increment in sulcal width, despite being associated to the thinning of cortex (as it implies an increment in the inter-gyral space), is not uniquely due to the latter, so that sulcal width can be an earlier, more efficient biomarker in discriminating converter MCI. Similarly better classification results of sulcal width with respect to cortical thickness was reported by Bertoux and colleagues [8], and this discrepancy between the two measures is worth of further investigation.

In the specific case of the prediction of MCI conversion, promising classification accuracies have been reported by using the sulcal width, mostly of temporal regions, as prime features [26, 27]. These studies, performed on cohorts of hundreds of patients, demonstrated that sulcal width can significantly improve classification performances of predictive models for MCI conversion. Nonetheless, it is particularly relevant to note that none of the above-mentioned

studies performed a quality control of the automatic sulcal labelling and, therefore, manual re-labelling of sulci. However, this may be a crucial step for an optimal identification of the specific sulci interested by the alterations. Pizzagalli and colleagues [30] demonstrated that the measures performed by the Morphologist software are not equally consistent across individuals for each sulcus and this is likely associated to the variability of the automatic labelling. The reduced list of sulci reliably estimated by Morphologist software, that the authors provide as a result of their study, does not include various sulci that resulted to be significant in our work, such as the inferior posterior temporal sulcus (S.T.i.post.), which was the best predictor of MCI conversion. Moreover, as stated above, the temporo-occipital and frontal regions, which overall are the mostly altered areas in our and in previous studies, are also those where the relabeling of sulci was most frequently needed. For example, Ficiarà and colleagues [26] found the width of the lateral occipito-temporal (S.O.T.lat.) sulcus and the superior temporal sulcus (S.T.s.) among the top discriminative features in their classifier, and these sulci were among the ones that most often required re-labelling for improving consistency across subjects.

Another interesting result that emerged from our study is that the best predictors of MCI conversion, such as the width of the S.T.i.post. were also capable of robustly discriminating cross-sectionally between cases with absent or mild symptoms of dementia compared to severe ones. This is in accord with previous results suggesting a progressive widening of temporal, frontal and parietal sulci with cognitive decline and dementia symptoms [8, 22, 24].

Our study confirms that degeneration in AD is not limited to limbic structure but appears in the early stage of converter MCI as sulcal modifications in temporo-occipital regions.

We also found a significant correlation of the sulcal width in the frontal lobes with cognitive performance in the MCI population. Specifically, wider left inferior precentral and right olfactory sulci were associated with worse performance in verbal short-term memory, while enlargement of the left olfactory sulcus correlated with lower performance in verbal long-term memory. Those data are consistent with previous fMRI studies reporting activation within frontal sulci (i.e., left inferior frontal sulcus) during language processes and working memory tasks [43]. Although the well-known association between the olfactory system and memory [44], to date,

no studies reported a specific association between olfactory sulci and long-term memory. Moreover, both verbal fluency and the ability to flexibly select and retrieve words (i.e., phonemic fluency performance) were negatively correlated with the right intermediate frontal sulcus' width. Those results are consistent with previous neuroimaging studies showing the involvement of right lateralized frontal areas in phonemic fluency task in HC [45] but also in AD and MCI patients [46].

Altogether, our results are aligned with those of previous studies showing a negative correlation of sulcal width with neuropsychological scores. For instance, Liu and colleagues [21] reported that wider sulcal spans reflect poorer cognitive performances, specifically in memory and language-related tasks. Bertoux and colleagues [8] found an association between verbal long-term memory and sulcal components of the frontal and temporal lobe as a whole, whereas the widening of frontal sulci was related to a decrease in executive functions.

This study presents some limitations. The first one is the size of the population investigated, which is relatively small in comparison to previous publications aiming to predict MCI conversion [26, 27], even though this allowed us to manually re-label sulci in all subjects giving the opportunity to explore the prognostic value of sulcal morphometry of sulci with high inter-subject variability. The 3D T1-weighted images were acquired with a field strength equal to 1.5 T, yet we expect these results to be reproducible on 3 T, as the achievable image quality can be comparable at the two field strengths, with the main difference being on the total acquisition time. Another potential limitation is the variable duration of the follow-up that may have an influence on the clinical outcome. Moreover, in this study, the non-converter MCI group size was smaller than the other subgroups. Because of this, an in-sample analysis, supported by a leave-one-out validation, was preferred to a further subdivision of the cohort into a training and test dataset. Finally, pathophysiological biomarkers were not available in this cohort of patients.

Conclusions

Sulcal morphometry emerged as a strong tool for differentiating HC, MCI sub-populations and AD. In particular, the sulcal width of different temporal, temporo-occipital and frontal sulci, whose reliability was established via visual quality control and eventual re-labelling, was demonstrated to be the best discriminating feature among the sulcal properties and also in comparison to other common morphological investigations. Although the size of population is limited, differently from studies with large size of population, in our study the data are acquired in the same site, thus avoiding possible bias due to interaction between sulcal measures and different MR sites. Our work gives an important added value to the previous analyses without manual relabeling, performed on large cohorts of patients, by confirming some results and showing other robust findings which could be further investigated in other populations. Our results are particularly promising in terms of the prediction of MCI conversion to AD, which was assessed in this work basing on a two-year clinical follow-up, and they support the use of sulcal width as a prognostic tool for this population.

AUTHOR CONTRIBUTIONS

Giovanni Sighinolfi (Conceptualization; Data curation; Formal analysis; Writing – original draft; Writing – review & editing); Micaela Mitolo (Conceptualization; Data curation; Writing – original draft; Writing – review & editing); Fabrizio Pizzagalli (Methodology; Writing – review & editing); Michelangelo Stanzani-Maserati (Writing – review & editing); Daniel Remondini (Writing – review & editing); Magali Jane Rochat (Writing – review & editing); Elena Cantoni (Writing – review & editing); Greta Venturi (Writing – review & editing); Gianfranco Vornetti (Writing – review & editing); Fiorina Bartiromo (Writing – review & editing); Sabina Capellari (Writing – review & editing); Rocco Liguori (Writing – review & editing); Caterina Tonon (Conceptualization; Supervision; Writing – original draft; Writing – review & editing); Claudia Testa (Conceptualization; Supervision; Writing – original draft; Writing – review & editing); Raffaele Lodi (Conceptualization; Supervision; Writing – original draft; Writing – review & editing).

ACKNOWLEDGMENTS

Decree No. 1553 of 11/10/2022 adopted by the Italian Ministry of University and Research "A multiscale integrated approach to the study of the nervous system in health and disease" (MNESYS).

CONFLICT OF INTEREST

Rocco Liguori, outside of the research carried out for this work, has royalties from Edra S.p.A. and has acted as paid advisor for Alexion Pharma Italy s.r.l., UCB Pharma S.p.A., Alfasigma s.r.l.; as paid relator for Summeet s.r.l., Alexion Pharma Italy s.r.l., Med Stage s.r.l., Amicus Therapeutics s.r.l.; as paid moderator for ECM Network s.r.l.

The other authors have no competing financial interests to disclose.

DATA AVAILABILITY

The numerical data that support the findings of this study will be made publicly available on the open access repository Zenodo (https://zenodo.org/) upon publication of this manuscript.

SUPPLEMENTARY MATERIAL

The supplementary material is available in the electronic version of this article: https://dx.doi.org/10.3233/JAD-231192.

REFERENCES

[1] Albert MS, DeKosky ST, Dickson D, Dubois B, Feldman HH, Fox NC, Gamst A, Holtzman DM, Jagust WJ, Petersen RC, Snyder PJ, Carrillo MC, Thies B, Phelps CH (2011) The diagnosis of mild cognitive impairment due to Alzheimer's disease: Recommendations from the National Institute on Aging-Alzheimer's Association workgroups on diagnostic guidelines for Alzheimer's disease. *Alzheimers Dement* **7**, 270-279.

[2] Borella E, Carretti B, Mitolo M, Zavagnin M, Caffarra P, Mammarella N, Fairfield B, Gamboz N, Piras F (2017) Characterizing cognitive inhibitory deficits in mild cognitive impairment. *Psychiatry Res* **251**, 342-348.

[3] Mitolo M, Stanzani-Maserati M, Capellari S, Testa C, Rucci P, Poda R, Oppi F, Gallassi R, Sambati L, Rizzo G, Parchi P, Evangelisti S, Talozzi L, Tonon C, Lodi R, Liguori R (2019) Predicting conversion from mild cognitive impairment to Alzheimer's disease using brain 1H-MRS and volumetric changes: A two-year retrospective follow-up study. *Neuroimage Clin* **23**, 101843.

[4] Mitolo M, Stanzani-Maserati M, Manners DN, Capellari S, Testa C, Talozzi L, Poda R, Oppi F, Evangelisti S, Gramegna LL, Magarelli S, Pantieri R, Liguori R, Lodi R, Tonon C (2021) The combination of metabolic posterior cingulate cortical abnormalities and structural asymmetries improves the differential diagnosis between primary progressive aphasia and Alzheimer's disease. *J Alzheimers Dis* **82**, 1467-1473.

[5] Liu T, Wen W, Zhu W, Kochan NA, Trollor JN, Reppermund S, Jin JS, Luo S, Brodaty H, Sachdev PS (2011) The relationship between cortical sulcal variability and cognitive performance in the elderly. *Neuroimage* **56**, 865-873.

[6] Jiang X, Zhang T, Zhang S, Kendrick KM, Liu T (2021) Fundamental functional differences between gyri and sulci: Implications for brain function, cognition, and behavior. *Psychoradiology* **1**, 23-41.

[7] Pini L, Pievani M, Bocchetta M, Altomare D, Bosco P, Cavedo E, Galluzzi S, Marizzoni M, Frisoni GB (2016) Brain atrophy in Alzheimer's disease and aging. *Ageing Res Rev* **30**, 25-48.

[8] Bertoux M, Lagarde J, Corlier F, Hamelin L, Mangin J-F, Colliot O, Chupin M, Braskie MN, Thompson PM, Bottlaender M, Sarazin M (2019) Sulcal morphology in Alzheimer's disease: An effective marker of diagnosis and cognition. *Neurobiol Aging* **84**, 41-49.

[9] Li S, Han Y, Wang D, Yang H, Fan Y, Lv Y, Tang H, Gong Q, Zang Y, He Y (2010) Mapping surface variability of the central sulcus in musicians. *Cereb Cortex* **20**, 25-33.

[10] Coyle TR, Kochunov P, Patel RD, Nery FG, Lancaster JL, Mangin J-F, Rivière D, Pillow DR, Davis GJ, Nicoletti MA, Serap Monkul E, Fox PT, Soares JC (2006) Cortical sulci and bipolar disorder. *Neuroreport* **17**, 1739-1742.

[11] Cachia A, Paillère-Martinot M-L, Galinowski A, Januel D, de Beaurepaire R, Bellivier F, Artiges E, Andoh J, Bartrés-Faz D, Duchesnay E, Rivière D, Plaze M, Mangin J-F, Martinot J-L (2008) Cortical folding abnormalities in schizophrenia patients with resistant auditory hallucinations. *Neuroimage* **39**, 927-935.

[12] Penttilä J, Paillére-Martinot M-L, Martinot J-L, Mangin J-F, Burke L, Corrigall R, Frangou S, Cachia A (2008) Global and temporal cortical folding in patients with early-onset schizophrenia. *J Am Acad Child Adolesc Psychiatry* **47**, 1125-1132.

[13] Penttilä J, Paillère-Martinot M-L, Martinot J-L, Ringuenet D, Wessa M, Houenou J, Gallarda T, Bellivier F, Galinowski A, Bruguière P, Pinabel F, Leboyer M, Olié J-P, Duchesnay E, Artiges E, Mangin J-F, Cachia A (2009) Cortical folding in patients with bipolar disorder or unipolar depression. *J Psychiatry Neurosci* **34**, 127-135.

[14] Penttilä J, Cachia A, Martinot J-L, Ringuenet D, Wessa M, Houenou J, Galinowski A, Bellivier F, Gallarda T, Duchesnay E, Artiges E, Leboyer M, Olié J-P, Mangin J-F, Paillère-Martinot M-L (2009) Cortical folding difference between patients with early-onset and patients with intermediate-onset bipolar disorder. *Bipolar Disord* **11**, 361-370.

[15] Mangin J-F, Rivière D, Duchesnay E, Cointepas Y, Gaura V, Verny C, Damier P, Krystkowiak P, Bachoud-Lévi A-C, Hantraye P, Remy P, Douaud G (2020) Neocortical morphometry in Huntington's disease: Indication of the

coexistence of abnormal neurodevelopmental and neurodegenerative processes. *Neuroimage Clin* **26**, 102211.

[16] Im K, Lee J-M, Won Seo S, Hyung Kim S, Kim SI, Na DL (2008) Sulcal morphology changes and their relationship with cortical thickness and gyral white matter volume in mild cognitive impairment and Alzheimer's disease. *Neuroimage* **43**, 103-113.

[17] Kochunov P, Mangin J-F, Coyle T, Lancaster J, Thompson P, Rivière D, Cointepas Y, Régis J, Schlosser A, Royall DR, Zilles K, Mazziotta J, Toga A, Fox PT (2005) Age-related morphology trends of cortical sulci. *Hum Brain Mapp* **26**, 210-220.

[18] Magnotta VA (1999) Quantitative *in vivo* measurement of gyrification in the human brain: Changes associated with aging. *Cereb Cortex* **9**, 151-160.

[19] Tang H, Liu T, Liu H, Jiang J, Cheng J, Niu H, Li S, Brodaty H, Sachdev P, Wen W (2021) A slower rate of sulcal widening in the brains of the nondemented oldest old. *Neuroimage* **229**, 117740.

[20] Kochunov P, Coyle T, Lancaster J, Robin DA, Hardies J, Kochunov V, Bartzokis G, Stanley J, Royall D, Schlosser AE, Null M, Fox PT (2010) Processing speed is correlated with cerebral health markers in the frontal lobes as quantified by neuroimaging. *Neuroimage* **49**, 1190-1199.

[21] Liu H, Zhang S, Jiang X, Zhang T, Huang H, Ge F, Zhao L, Li X, Hu X, Han J, Guo L, Liu T (2019) The cerebral cortex is bisectionally segregated into two fundamentally different functional units of gyri and sulci. *Cereb Cortex* **29**, 4238-4252.

[22] Mortamais M, Gutierrez L-A, Balem M, Bars EL, de Champfleur NM, Bouyahia A, Chupin M, Perus L, Fisher C, Vellas B, Andrieu S, Mangin J-F, Berr C, Gabelle A (2022) Sulcal morphology as cognitive decline predictor in older adults with memory complaints. *Neurobiol Aging* **113**, 84-94.

[23] Cai K, Xu H, Guan H, Zhu W, Jiang J, Cui Y, Zhang J, Liu T, Wen W (2017) Identification of early-stage Alzheimer's disease using sulcal morphology and other common neuroimaging indices. *PLoS One* **12**, e0170875.

[24] Hamelin L, Bertoux M, Bottlaender M, Corne H, Lagarde J, Hahn V, Mangin J-F, Dubois B, Chupin M, de Souza LC, Colliot O, Sarazin M (2015) Sulcal morphology as a new imaging marker for the diagnosis of early onset Alzheimer's disease. *Neurobiol Aging* **36**, 2932-2939.

[25] Liu T, Sachdev PS, Lipnicki DM, Jiang J, Cui Y, Kochan NA, Reppermund S, Trollor JN, Brodaty H, Wen W (2013) Longitudinal changes in sulcal morphology associated with late-life aging and MCI. *Neuroimage* **74**, 337-342.

[26] Ficiara E, Crespi V, Gadewar SP, Thomopoulos SI, Boyd J, Thompson PM, Jahanshad N, Pizzagalli F (2021) Predicting progression from mild cognitive impairment to Alzheimer's disease using MRI-based cortical features and a two-state Markov Model. In *2021 IEEE 18th International Symposium on Biomedical Imaging (ISBI)* IEEE, Nice, France, pp. 1145-1149.

[27] Plocharski M, Østergaard LR (2019) Prediction of Alzheimer's disease in mild cognitive impairment using sulcal morphology and cortical thickness. In *World Congress on Medical Physics and Biomedical Engineering 2018*, Lhotska L, Sukupova L, Lacković I, Ibbott GS, eds. Springer Nature Singapore, Singapore, pp. 69-74.

[28] Petersen RC (2004) Mild cognitive impairment as a diagnostic entity. *J Intern Med* **256**, 183-194.

[29] McKhann GM, Knopman DS, Chertkow H, Hyman BT, Jack CR, Kawas CH, Klunk WE, Koroshetz WJ, Manly JJ, Mayeux R, Mohs RC, Morris JC, Rossor MN, Scheltens P, Carrillo MC, Thies B, Weintraub S, Phelps CH (2011) The diagnosis of dementia due to Alzheimer's disease: Recommendations from the National Institute on Aging-Alzheimer's Association workgroups on diagnostic guidelines for Alzheimer's disease. *Alzheimers Dement* **7**, 263-269.

[30] Pizzagalli F, Auzias G, Yang Q, Mathias SR, Faskowitz J, Boyd JD, Amini A, Rivière D, McMahon KL, de Zubicaray GI, Martin NG, Mangin J-F, Glahn DC, Blangero J, Wright MJ, Thompson PM, Kochunov P, Jahanshad N (2020) The reliability and heritability of cortical folds and their genetic correlations across hemispheres. *Commun Biol* **3**, 510.

[31] Dojat M, Pizzagalli F, Hupé J-M (2018) Magnetic resonance imaging does not reveal structural alterations in the brain of grapheme-color synesthetes. *PLoS One* **13**, e0194422.

[32] Geffroy D, Rivière D, Denghien I, Souedet N, Laguitton S, Cointepas Y (2011) BrainVISA: A complete software platform for neuroimaging. In *Python in Neuroscience workshop*, Paris.

[33] Fischer C, Operto G, Laguitton S, Perrot M, Denghien I, Rivière D, Mangin J-F (2012) Morphologist 2012: The new morphological pipeline of BrainVISA. *Proc HBM*.

[34] Perrot M, Rivière D, Mangin J-F (2011) Cortical sulci recognition and spatial normalization. *Med Image Anal* **15**, 529-550.

[35] Mangin J-F, Riviere D, Cachia A, Duchesnay E, Cointepas Y, Papadopoulos-Orfanos D, Collins DL, Evans AC, Regis J (2004) Object-based morphometry of the cerebral cortex. *IEEE Trans Med Imaging* **23**, 968-982.

[36] Pizzagalli F, Auzias G, Kochunov P, Faskowitz JI, McMahon KL, De Zubicaray GI, Martin NG, Wright MJ, Jahanshad N, Thompson PM (2016) Genetic analysis of cortical sulci in 1,009 adults. In *2016 IEEE 13th International Symposium on Biomedical Imaging (ISBI)* IEEE, Prague, Czech Republic, pp. 833-837.

[37] Mangin J-F, Rivière D, Cachia A, Duchesnay E, Cointepas Y, Papadopoulos-Orfanos D, Scifo P, Ochiai T, Brunelle F, Régis J (2004) A framework to study the cortical folding patterns. *Neuroimage* **23**, S129-S138.

[38] Segal E, Petrides M (2012) The morphology and variability of the caudal rami of the superior temporal sulcus: Caudal rami of the STS. *Eur J Neurosci* **36**, 2035-2053.

[39] Desikan RS, Ségonne F, Fischl B, Quinn BT, Dickerson BC, Blacker D, Buckner RL, Dale AM, Maguire RP, Hyman BT, Albert MS, Killiany RJ (2006) An automated labeling system for subdividing the human cerebral cortex on MRI scans into gyral based regions of interest. *Neuroimage* **31**, 968-980.

[40] Voevodskaya O, Simmons A, Nordenskjöld R, Kullberg J, Ahlström H, Lind L, Wahlund L-O, Larsson E-M, Westman E, Alzheimer's Disease Neuroimaging Initiative (2014) The effects of intracranial volume adjustment approaches on multiple regional MRI volumes in healthy aging and Alzheimer's disease. *Front Aging Neurosci* **6**, 264.

[41] Unal I (2017) Defining an optimal cut-point value in ROC analysis: An alternative approach. *Comput Math Methods Med* **2017**, 3762651.

[42] Tenenbaum JB, Silva V de, Langford JC (2000) A global geometric framework for nonlinear dimensionality reduction. *Science* **290**, 2319-2323.

[43] Ruland SH, Palomero-Gallagher N, Hoffstaedter F, Eickhoff SB, Mohlberg H, Amunts K (2022) The inferior frontal

sulcus: Cortical segregation, molecular architecture and function. *Cortex* **153**, 235-256.

[44] Wilson DA, Best AR, Sullivan RM (2004) Plasticity in the olfactory system: Lessons for the neurobiology of memory. *Neuroscientist* **10**, 513-524.

[45] Zhang Y, Zhang J, Oishi K, Faria AV, Jiang H, Li X, Akhter K, Rosa-Neto P, Pike GB, Evans A, Toga AW, Woods R, Mazziotta JC, Miller MI, van Zijl PCM, Mori S (2010) Atlas-guided tract reconstruction for automated and comprehensive examination of the white matter anatomy. *Neuroimage* **52**, 1289-1301.

[46] Clark DG, Wadley VG, Kapur P, DeRamus TP, Singletary B, Nicholas AP, Blanton PD, Lokken K, Deshpande H, Marson D, Deutsch G (2014) Lexical factors and cerebral regions influencing verbal fluency performance in MCI. *Neuropsychologia* **54**, 98-111.